Journal of Fluorescence, Vol. 11, No. 3, September 2001 (© 2001)

Detection and Characterization of Membrane Microheterogeneity by Resonance Energy Transfer

Luís M. S. Loura,[1,2] Rodrigo F. M. de Almeida,[1] and Manuel Prieto[1,3]

The application of resonance energy transfer (RET) in the study of heterogeneity in membrane systems is described. Useful formalisms for monophasic and biphasic systems are presented, together with quantitative studies. Evidence for reduction of dimensionality, probe segregation, and microdomain sizes in these systems is discussed. Selected examples of multicomponent systems (natural membranes or model systems including proteins) are also referred, as well as recent work using RET under the microscope.

KEY WORDS: Energy transfer; lipid domain; membranes; phase separation.

INTRODUCTION

The traditional picture of the lipid bilayer of biological membranes as proteins embedded in a structureless lipid environment [1] is nowadays viewed as incorrect, as a result of research carried out in the last decades. Although lipid domains with sizes in the micrometer range may be visualized directly, the membrane dynamical organization in the nanometer scale (probably relevant to the biological function of membrane proteins) is much more difficult to study experimentally [2]. In this respect, spectroscopic techniques, namely, fluorescence, are among the few available tools. The use of fluorescence techniques in the study of membrane heterogeneity was reviewed recently [3], with focus on probe properties such as fluorescence anisotropy, quantum yield and lifetime, and their variation as a function of the lipid system composition. However, approaches based on the phenomenon of resonance energy transfer (RET [4]) were not considered.

Given its unique features (namely, the strong dependence of the transfer rate on the distance and local concentration), it is surprising that the number of quantitative (especially time-resolved) studies of RET in detection and characterization of lipid distribution heterogeneity and phase separation are so few. RET was identified as a promising technique for the study of phase separation in membranes more than two decades ago [5]. In fact, due to the relatively short lifetimes of the excited states of most fluorophores (~1–10 ns), RET is one of the best available techniques to reveal the smallest nanoscale membrane domains [6].

This article describes the application of RET methodologies to the study of heterogeneity in membrane systems. The following points are addressed.

(i) The work carried out in cuvettes, at variance with experiments under the microscope, allows high-quality quantitative data to be obtained, which is an essential requisite for model applications. These methodologies are presented in detail and applied to both mono- and biphasic model membrane systems. Evidence for reduction of dimensionality, probe segregation, and microdomain sizes is discussed.

(ii) Some relevant studies regarding the topology of multicomponent systems (e.g., including

[1] Centro de Química-Física Molecular, Instituto Superior Técnico, P-1049-001 Lisboa, Portugal.
[2] Departamento de Química, Universidade de Évora, Rua Romão Ramalho, 59, P-7000-671 Évora, Portugal.
[3] To whom correspondence should be addressed. Fax: +351 218464455. E-mail: prieto@alfa.ist.utl.pt

1053-0509/01/0900-0197$19.50/0

proteins) are described. Preference was given to those in which quantitative information is sought.

(iii) Due to its relevance, some recent RET work carried under the microscope is also mentioned. For this purpose, those addressing the structure of sphingolipid–cholesterol–glycosylphosphatidylinositol (GPI)-anchored protein-enriched domains ("rafts") were chosen, due to the recent interest on this type of aggregates.

Outside the scope of this review are works using energy migration (homotransfer), as well as studies of RET in the rapid diffusion limit.

THEORY OF RET TO RANDOMLY DISTRIBUTED ACCEPTORS

The kinetics of RET were originally derived by Förster [7]. The rate of energy transfer between a donor molecule, with fluorescence lifetime τ, and an acceptor molecule, separated by a distance R, is given by

$$k_T = \frac{1}{\tau}\left(\frac{R_0}{R}\right)^6 \tag{1}$$

where R_0 is the critical distance, which can be calculated from

$$R_0 = 0.2108 \cdot \left[\kappa^2 \cdot \Phi_D \cdot n^{-4} \cdot \int_0^\infty I(\lambda) \cdot \epsilon(\lambda) \cdot \lambda^4 \cdot d\lambda\right]^{1/6} \tag{2}$$

where in turn κ^2 is the orientation factor (see Ref. 4 for a detailed discussion), Φ_D is the donor quantum yield in the absence of acceptor, n is the refractive index, λ is the wavelength, $I(\lambda)$ is the normalized donor emission spectrum, and $\epsilon(\lambda)$ is the acceptor molar absorption spectrum. As is clear from Eq. (2), R_0 can be calculated from spectroscopic data. If the λ units used in Eq. (2) are nanometers, then the calculated R_0 has units of angstroms.

If the same donor molecule is now surrounded by N_A acceptors (R_i being the distance between the donor and the acceptor molecule i) and R_0 is the same for every donor–acceptor pair, the time-resolved fluorescence decay $i_{DA}(t)$ can be described by

$$i_{DA}(t) = \exp\left(-\frac{t}{\tau}\right) \prod_{i=1}^{N_A} \exp\left[\left(-\frac{t}{\tau}\right)\left(\frac{R_0}{R_i}\right)^6\right] \tag{3}$$

Under these conditions, one must calculate the product on the right, which can be replaced by integration assuming a random distribution of acceptors. This procedure is also valid if there is a distribution of equivalent donors. The result for an infinite two-dimensional system (*cis* RET geometry; see Fig. 1), assuming that there is no homotransfer between donors, the fraction of excited acceptors is negligible, translational diffusion is negligible, and the exclusion distance between donors and acceptors is much smaller than R_0, is

$$i_{DA,cis}(t) = \exp(-(t/\tau) - ct^{1/3}) \tag{4}$$

where

$$c = \Gamma(2/3) \cdot n \cdot \pi \cdot R_0^2 \cdot \tau^{-1/3} \tag{5}$$

In this equation, n is the surface density of acceptors and Γ is the complete gamma function. The same approach can be used to obtain the decay for a system where donors and acceptors are located in infinite parallel planes (*trans* RET geometry; see Fig. 1), separated by a distance H, with the same assumptions. The result is [8]

$$i_{DA,trans}(t) = \exp\left\{-\frac{t}{\tau} - \frac{2c}{\Gamma(2/3) \cdot b} \int_0^1 [1 - \exp(-t\, b^3\, \alpha^6)]\alpha^{-3}\, d\alpha\right\} \tag{6}$$

In this equation, $b = (R_0/H)/\tau^{1/3}$. In either case, the RET efficiency (useful in analysis of steady-state data) is defined by

$$E = 1 - \int_0^\infty i_{DA}(t)dt \Big/ \int_0^\infty i_D(t)dt \tag{7}$$

where $i_D(t)$ is the donor decay in the absence of acceptor.

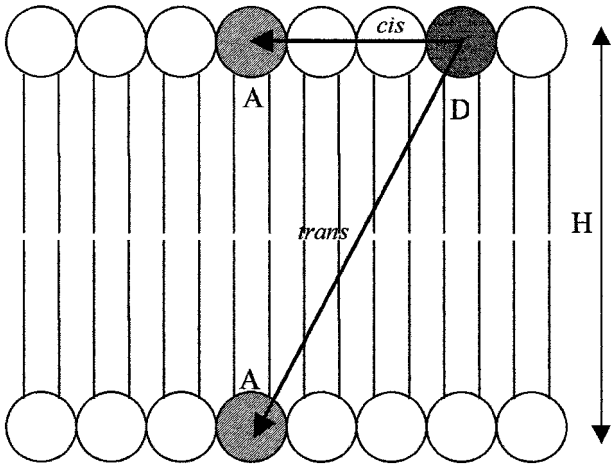

Fig. 1. Schematic representation of the *cis* and *trans* RET geometries referred to in the text. D, donor probe; A, acceptor probe; H, distance between opposite planes of location of probes.

The integration can be carried out analytically [9] but, especially for *trans* transfer or multiexponentially decaying donors (as often is the case in model membranes), is best done numerically.

APPLICATIONS TO ONE-PHASE LIPID SYSTEMS

In the past 25 years, several authors have tried to analyze RET data in model membranes using variations of Eqs. (4)–(6) (time-resolved data) or (7) (steady-state data). In their pioneering work, Fung and Stryer [10] studied RET between fluorescently labeled phosphatidylethanolamine (PE) in large unilamellar vesicles (LUV) of phosphatidylcholine (PC) from egg yolk. Although from the variation of steady-state RET efficiency data with acceptor concentration it was possible to recover R_0 values in accordance with those obtained spectroscopically, the donor decay curves are considerably different from the theoretical ones, pointing to a nonrandom probe distribution. Studies by other authors have also revealed deviations between the observed donor decays and the theoretical expectations for two-dimensional geometry in RET between dyes in one-component gel phase vesicles [11–13]. RET between monomers and dimers of acylated rhodamine dyes in phosphatidic acid (PA) Langmuir–Blodgett multilayers also revealed unsatisfactory matching to the theoretical framework (e.g., Ref. 14). However, in the latter example, the authors were able to fit globally the donor decays to a modified version of Eq. (4):

$$i_{DA,cis}(t) = (1 - \alpha)\exp(-(t/\tau) - ct^{1/3}) + \alpha \cdot \exp(-(t/\tau)) \qquad (8)$$

This equation assumes that a fraction α of the donors might be "isolated" regarding RET (in practice, having no acceptor molecules within a distance of $2R_0$) and show the same decay as in the absence of acceptor.

More recent studies of RET between lipophilic probes in fluid-phase unilamellar vesicles have been carried out, showing accordance between experimental and theoretical decays. From time-resolved data of RET from *N*-(7-nitrobenz-2-oxa-1,3-diazol-4-yl) (NBD)-16:0,16:0 PE (*m*:*n* denotes a chain with *m* carbon atoms and *n* double bonds) to *N*-(lissamine–rhodamine B) (Rh)-16:0,16:0 PE in 18:1,18:1 PC [15], a linear dependence of the recovered *c* parameter as a function of the acceptor concentration was verified, as expected from Eq. (5), allowing the calculation of the area per lipid molecule. This dependence was also verified in RET from octadecylrhodamine B (ORB) to 1,1′,3,3,3′,3′-hexamethylindotricarbocyanine [$DiIC_1(7)$] in fluid 16:0,16:0 PC LUV [16]. In this study, a modified Eq. (4) was derived for biexponentially decaying donors, and the decays were globally analyzed, with linkage of donor lifetimes and preexponential ratio (Fig. 2). However, analysis of the decays for the same system but below the main transition temperature was not successful, pointing to probe aggregation in the gel phase, possibly in line defects in the gel-phase structure. In this situation, the traditional framework, derived assuming a random distribution of probes, is no longer valid.

A RET formalism that allows the possibility of a nonrandom probe distribution is the mean acceptor concentration model [17]. It takes into account a continuous probability function $f(c)$ of having donors with a mean local concentration c of acceptors in their surroundings, rather than a discrete function characterized by probability α of "seeing" no acceptors and probability 1-α of sensing a concentration c, expressed by Eq. (8). In this model Eq. (4) is locally valid and the decay law is expressed as a Fredholm integral equation of the first kind regarding recovery of the function $f(c)$:

$$i_{DA}(t) = \int_0^\infty f(c) \cdot \exp(-(t/\tau) - ct^{1/3}) \cdot dc \qquad (9)$$

There are two problems associated with this method. First, although it is an obvious improvement over the step-function model expressed by Eq. (8), in its derivation it is implicitly assumed that each donor is surrounded by a uniform concentration of acceptors. It is therefore not a priori obvious whether it is applicable in the case of spatial nonhomogeneity. Second, the solution of Eq. (9) leads to an ill-conditioned problem, meaning that small errors in $i_{DA}(t)$ may result in large changes in the recovered $f(c)$. Having this in consideration, the model was tested through two types of simulations [18]:(1) artificial decays were generated for nonrandom probe distributions by Monte Carlo simulations and then analyzed using Eq. (9), and (2) exact decay curves were convoluted with an instrumental response function, and then Poisson noise was added unto them, to simulate "rough" experimental decay data. These experimental-like decays were then globally analyzed with software based on the Marquardt algorithm [19]. It was concluded that, for the simulated configurations (two distinct populations of donors, surrounded by different local acceptor concentrations), the mean concentration model, with a sum of two Gaussian curves for the acceptor concentration distribution $f(c)$, gave an adequate description of the RET kinetics.

This model was then used to analyze the time-resolved RET data for the pairs ORB/$DiIC_1(7)$ and NBD-

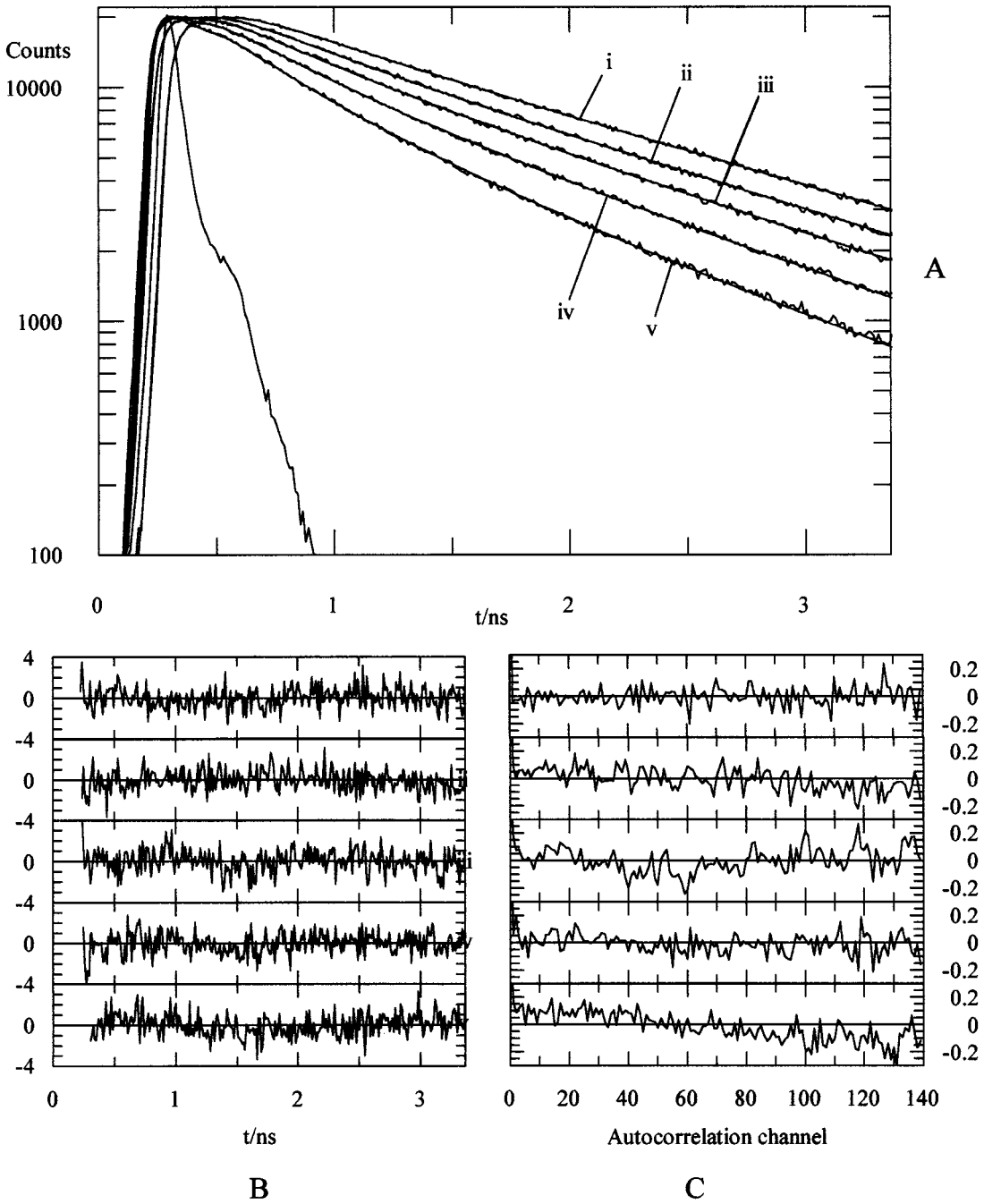

Fig. 2. (A) Time-resolved fluorescence intensity of ORB in fluid-phase (50°C) 16:0,16:0 PC LUV for different $DilC_l(7)$ concentrations. $DilC_l(7)$-to-outer leaflet 16:0,16:0 PC LUV ratio: (i) 0; (ii) 0.0022; (iii) 0.0044; (iv) 0.0082; (v) 0.0126. The laser pulse profile is represented, and the smooth lines are best-fit curves (global analysis) of the RET formalism of a random distribution of probes in one phase. (B) Weighted residuals plots. (C) Autocorrelation function plots. Reprinted with permission from Ref. 16. Copyright 1996 Biophysical Society.

16:0,16:0 PE/Rh-16:0,16:0 PE [20] in both fluid- and gel-phase 16:0,16:0 PC LUV. For both pairs, narrow unimodal $f(c)$ were recovered for the fluid phase and moderate acceptor overall concentrations, confirming the random distribution of probes in this system. Higher overall acceptor concentrations (>1 mol%) resulted in wider (but still unimodal) distributions, revealing a small degree of acceptor aggregation (Fig. 3E, top).

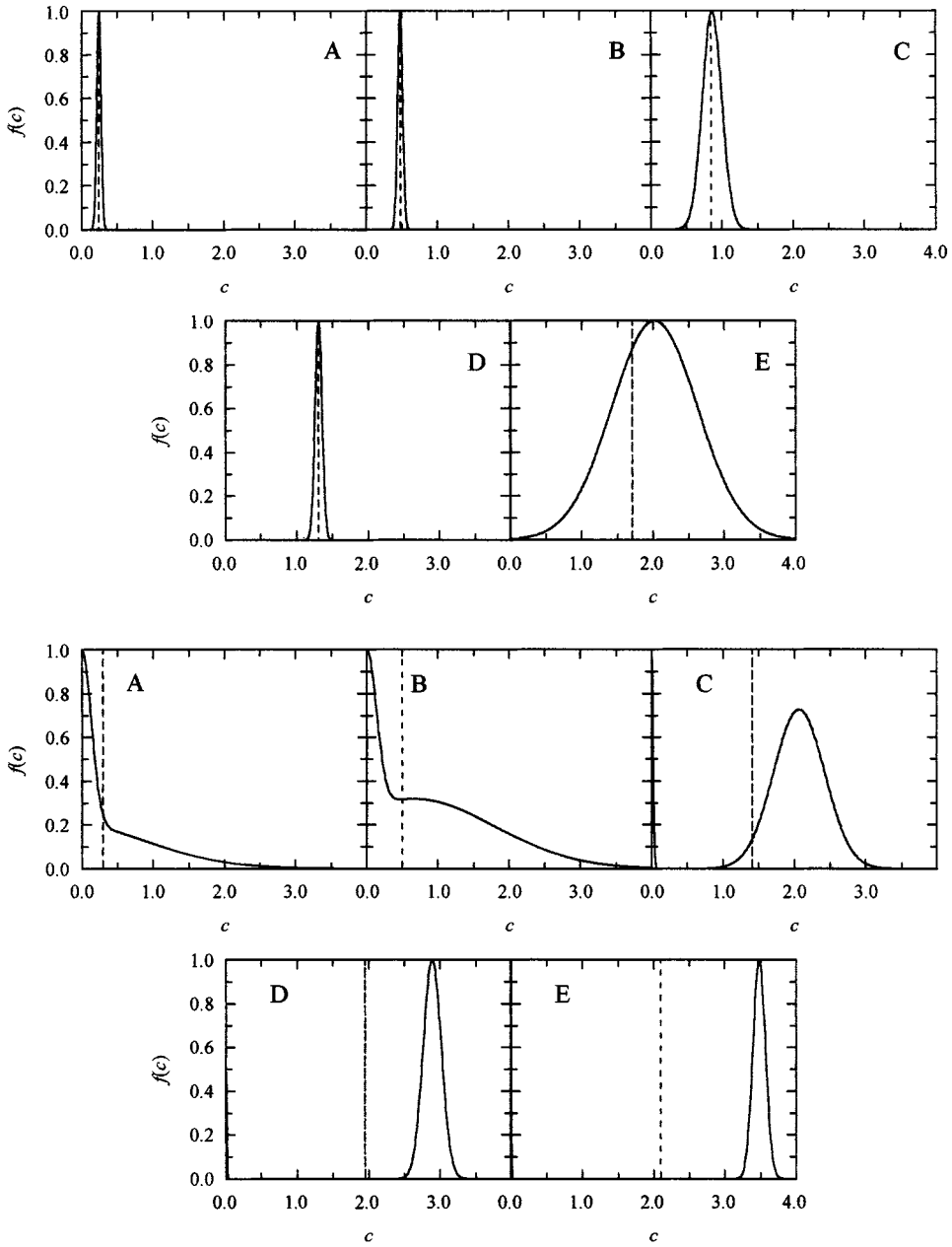

Fig. 3. Solid lines: acceptor concentration distributions recovered for ORB decay data in 16:0,16:0 PC LUV in the presence of different amounts of $DilC_I(7)$. Ratios of $DilC_I(7)$ to outer leaflet 16:0,16:0 PC: *A*, 0.0022; *B*, 0.0044; *C*, 0.0082; *D*, 0.0126; *E*, 0.0171. Vertical dashed lines: *c* values recovered for the random distribution fit [Eq. (4)]. Top plots: $T = 50°C$ (fluid-phase LUV). Bottom plots: $T = 25°C$ (gel-phase LUV). Reprinted with permission from Ref. 20. Copyright 2000 American Chemical Society.

The striking results came in the analysis of gel-phase data. In this case, bimodal $f(c)$ (centered around finite c values) were recovered for all acceptor concentrations for the NBD-16:0,16:0 PE/Rh-16:0,16:0 PE pair. This was interpreted in terms of partial segregation of both donor and acceptor probes to the line defects of the gel structure. The high local concentration peak would then correspond to donors located in this environment that would sense a larger local acceptor concentration. From the location of the peaks and their intensity one is able to estimate a "partition coefficient" of the probes for the defect pseudo-phase (see next section for details on the

calculation). $K_p \approx 10$ is observed for both probes, denoting the preference of the probes for the defects, where they possibly can be better accommodated than inside the bulk gel lattice. However, the K_p values decrease for higher overall acceptor concentrations, probably meaning that the available defect sites become saturated with probe molecules.

For the ORB/DiIC$_1$(7) pair, a different trend was observed: $f(c)$ evolved from a distribution with a maximum at $c = 0$, for a low overall acceptor concentration, to a unimodal distribution centered at higher c values (see Fig. 3, bottom). No evidence for donor aggregation was observed in a study of emission depolarization by homotransfer. The variation in the recovered $f(c)$ was thus ascribed to acceptor segregation in the defect lines. For a low overall acceptor concentration, a large fraction of this probe would be located in the defects, leaving a sizable proportion of donors as "isolated" in RET terms (peak at $c \approx 0$). For a higher overall acceptor concentration, as more acceptor molecules are incorporated, a saturation effect similar to that of the NBD-16:0,16:0 PE/Rh-16:0,16:0 PE pair probably occurs in the defects, significant amounts of acceptor are incorporated in the bulk gel lattice and gradually fewer donors remain isolated. These conclusions are supported by additional photophysical measurements (steady-state energy transfer, fluorescence self-quenching in steady and transient states, and energy migration) and agree with the mentioned Monte Carlo simulations. This analysis methodology was also used in the RET study of interactions between the fluorescent sterol dehydroergosterol and the polyene antibiotic filipin in small unilamellar vesicles of 16:0,16:0 PC [21], revealing the formation of both filipin–sterol and filipin–filipin aggregates.

APPLICATIONS TO TWO-PHASE LIPID SYSTEMS

In these systems, as long as the donor and acceptor probes prefer one of the two coexisting phases, RET is obviously sensitive to phase separation. For example, if the two probes show preference for the same phase, most donors will be located in a region enriched with acceptor, and it can be shown that RET efficiency increases accordingly. The opposite effect is verified if the probes partition to distinct phases. Thus, in biphasic systems, RET efficiency and probe partition are closely related. For a planar system with lateral phase separation (two infinite phases), the donor decay in the presence of acceptor is given by [22]

$$i_{DA,cis}(t) = A_1\exp(-t/\tau_1)\exp(-c_1 t^{1/3}) + A_2\exp(-t/\tau_2)\exp(-c_2 t^{1/3}) \quad (10)$$

where τ_i is the donor excited-state lifetime in phase i (i = 1,2), and c_i is given by Eq. (5), replacing τ with τ_i, n with n_i (the acceptor surface density in phase i), and R_0 with R_{0i}, the critical RET distance for pure phase i. It is assumed that the probe distribution is random inside each phase (nonrandomness could be rationalized in the framework of the mean concentration model; however, that would lead to a fitting equation with a very large number of parameters for biphasic systems). The preexponential A_i is proportional to the number of donor molecules in phase i. The donor decay in the absence of acceptor is simply

$$i_D(t) = A_1\exp(-t/\tau_1) + A_2\exp(-t/\tau_2) \quad (11)$$

In practice, the donor may decay biexponentially in both pure phases, and the RET geometry may not be strictly planar (*cis* geometry in Fig. 1), because donors located in one bilayer leaflet may be able to transfer its excitation energy to acceptors located on the opposite monolayer. The necessary changes for these situations have been described [22]. In any case, the recovered parameters contain information relative to the amount of donor and acceptor in each phase. The partition coefficient of a probe between phase 1 and phase 2 is given by (e.g., Ref. 3)

$$K_p = (P_2/X_2)/(P_1/X_1) \quad (12)$$

where P_1 is the probe mole fraction in lipid phase 1, and X_1 is the lipid phase 1 mole fraction (therefore $P_2 = 1 - P_1$ and $X_2 = 1 - X_1$). It is easy to show that the partition coefficients of donor (K_{pD}) and acceptor (K_{pA}) probes can be calculated straightforwardly from the RET decay parameters:

$$K_{pD} = (A_2/X_2)/(A_1/X_1) \quad (13)$$

$$K_{pA} = (c_2 \cdot a_2)/(c_1 \cdot a_1) \quad (14)$$

where a_i is the area per lipid molecule in phase i.

Now let x represent the overall mole fraction of the lipid component which predominates in phase 2 at a given temperature, and let the phase coexistence boundaries at this temperature be x_1 ($X_2 = 0$) and x_2 ($X_2 = 1$). If at a given temperature X_1 are known for two points, $A(x_A, T)$ and $B(x_B, T)$, which are known to be located inside the phase coexistence range, x_1 and x_2, are given by [22]

$$x_1 = (x_A \cdot X_{2B} - x_B \cdot X_{2A})/(X_{1A} - X_{1B}) \quad (15)$$

$$x_2 = (x_B \cdot X_{1A} - x_A \cdot X_{1B})/(X_{1A} - X_{1B}) \quad (16)$$

which allows one to calculate the compositions of phases 1 and 2 at that temperature from time-resolved RET data. If this procedure is repeated for several temperatures, the phase diagram is obtained.

These simple relationships are strictly valid only for very large domains ($\gg R_0$). To test this formalism for a situation of phase separation into small domains, synthetic decays were generated by Monte Carlo simulation and then globally analyzed (in the presence and absence of acceptor) using Eqs. (10) and (11). It was verified that even for domain size $\approx 3.5R_0$ ($\approx$15–20 nm for most current RET pairs), satisfactory phase boundaries estimates are recovered, whereas the K_{pA} values calculated using Eqs. (13) and (14) are closer to unity than the input values. That is, if the acceptor prefers to incorporate in the minority phase 1 ($K_{pA} < 1$), but the domains of this phase are very small, donors inside those domains are still sensitive to the region outside them and "see" a local concentration of acceptor which is smaller than the domain value c_1. The opposite happens for donors outside the domains. As a consequence, c_1 is underestimated, c_2 is overestimated, and K_{pA} calculated from Eq. (14) is overestimated. Conversely, if $K_{pA} > 1$, but the domains of phase 1 are very small, K_{pA} calculated from time-resolved RET parameters is understimated.

Of course, K_p values can be obtained by a plethora of established methods, including other photophysical techniques [3]. The uniqueness of RET in this respect resides in the dependence of the "apparent K_p," the value recovered after analysis, on the size of the phases. Other fluorescent properties often used for calculation of K_p, such as fluorescence intensity, lifetime, and anisotropy, are dependent only on the immediate environment of the probe (at least for common dyes, with lifetimes shorter than 10 ns) and are insensitive to the domain size. In this way, a procedure for obtaining information on the size of membrane domains would be the following.

(i) Measure K_p by distance-independent methods.
(ii) Obtain time-resolved RET data and calculate K_{pA} from global analysis.
(iii) Compare the K_{pA} values obtained in i and ii and, from their eventual difference, make conclusions about domain sizes.
(iv) This would allow an "educated guess," which could in turn be confirmed from adequate Monte Carlo simulations. Theoretical decay laws would thus be obtained and compared with the experimental ones.

This discussion is valid for all biphasic systems. Experimentally, one can distinguish between gel/fluid and fluid/fluid phase separation types. Gel/fluid heterogeneity was studied in a recent steady-state RET work, in 16:0,16:0 PC/18:0,22:6 PC mixtures [23]. The effect of cholesterol in mixtures of 18:0,18:1 PC/18:0,22:6 PC mixtures was also investigated. NBD-PE and Rh-PE probes with two saturated, two unsaturated, or one saturated and one unsaturated acyl chains were used as RET probes. In this qualitative work, some important questions were not addressed, e.g., the fact that neither R_0 nor (most importantly) the area/lipid molecule is the same in the two coexisting phases. In particular, the very large effect of cholesterol upon the area/lipid molecule in the fluid phase, tending to increase the RET efficiency, may mask subtle variations due to differences in partition and must be taken into account.

In another gel/fluid heterogeneity study [24], mixtures of 12:0,12:0 PC/18:0,18:0 PC were investigated for two temperatures and compositions inside the phase coexistence range. The short-tailed RET donor, NBD-12:0,12:0 PE, and a short-tailed RET acceptor, 1,1′-didodecil-3,3,3′,3′-tetramethylindocarbocyanine [$DiIC_{12}$(3)], were shown to prefer the fluid phase (rich in short-tailed phospholipid) by both intrinsic anisotropy, lifetime, and RET measurements, in agreement with published reports. The other studied RET acceptor, long-tailed proble 1,1′-dioctadecil-3,3,3′,3′-tetramethylindocarbocyanine [$DiIC_{18}$(3)], was expected to perfer to gel (rich in long-tailed phospholipid), on account of hydrophobic matching considerations [25]. While intrinsic lifetime studies indeed indicated preferential partition of $DiIC_{18}$(3) into a rigidified environment, RET analysis pointed to an increased donor–acceptor proximity as a consequence of phase separation. These apparently conflicting results were rationalized on the basis of segregation of $DiIC_{18}$(3) to the gel/fluid interphase. To fluid-located donors sense these interphase-located acceptors, fluid domains should be small (not exceed ~10–15 nm). This work shows that membrane probes which apparently prefer the gel phase may show a nonrandom distribution in this medium (in agreement with the study described above for pure DPPC gel phase LUV) and tend to locate in an environment which simultaneously leads to less strict packing constraints and to favorable hydrophobic matching interactions.

For fluid/fluid heterogeneities, which are traditionally most difficult to characterize, these packing problems are certainly less critical. One may distinguish between fluid/fluid phospholipid heterogeneity (mixtures of two structurally different phospholipids above the main temperatures of both) and liquid disordered (ld)/liquid ordered (lo) heterogeneity (e.g., PC/cholesterol mixtures). Although both types are certainly relevant as models of biomembrane heterogeneity, very few RET studies have

been carried out regarding either of them. In one steady-state work [26], the RET efficiency between the excimer of 16:0,1-pyrenedecanoyl PC and 4,4-difluoro-5-methyl-4-boro-3*a*,4*a*-diaza-*s*-indacene-3-dodecanoyl,16:0 PC was studied as a function of composition for mixed 16:0,18:1 PC/16:0,18:1 phosphatidylglycerol (PG), 16:0,18:1 PC/16:0,18:1 phosphatidylserine, and 16:0,18:1 PC/16:0,18:1 PA LUV, at 35°C (above the main transition temperatures of all the lipids used). It was verified that E increases continuously with the amount of anionic phospholipid, but while variations in 16:0,18:1 PC/16:0,18:1 PG LUV were small, the increase in RET efficiency was very significant in the other systems (especially in the 16:0,18:1 PC/16:0/18:1 PA mixtures). These observations point to preferred colocalization of the labeled PC probes and to probable fluid–fluid phase separation.

Regarding lo/ld heterogeneity, two studies were recently carried out in the 14:0,14:0 PC/cholesterol system. The phase diagram for this mixture has been determined [27]. The main focus was to probe the small domains using the strategy outlined above. In one study [28], 22–NBD-23,24-bisnor-5-colen-3β-ol (NBD-cholesterol) was used as donor and ORB was used as acceptor. It was expected that NBD-cholesterol would mimic the behavior of cholesterol and partition preferably to the lo phase. However, using both steady-state fluorescence and time-resolved RET, values much less than unity were obtained for the lo/ld partition coefficients for both probes, pointing to a preference for the cholesterol-poor phase. It is concluded that, in particular, NBD-cholesterol is not a suitable cholesterol analogue and its distribution behavior in PC/cholesterol bilayers is in fact opposite to that of cholesterol. However, additional photophysical measurements revealed that both probes aggregate in the lo phase, preventing further characterization of the lipid domain structure.

In the other study [22], NBD-14:0,14:0 PE and Rh-14:0,14:0 PE were used as donor and acceptor, respectively. Although Rh-14:0,14:0 PE prefers the ld phase, the opposite is observed for NBD-14:0,14:0 PE, as determined by fluorescence intensity and anisotropy variations, respectively. Accordingly, RET efficiency decreases as a consequence of phase separation (see Fig. 4A). Figure 4B shows the theoretical [obtained from Eq. (5) and using the size-independent K_{pA} values] and the experimental c_i ($i = \alpha$ for ld, β for lo) inside the phase coexistence range. For $x_{chol} = 0.15$ and $x_{chol} = 0.20$ (the studied samples with smaller X_β in the lo/ld coexistence range), the experimental c_α value (which would always be expected to be larger than c_β) is smaller than expected, while the opposite is true for c_β. This, together with Monte Carlo simulations of decays in biphasic systems, suggests that in this region of the phase diagram, the lo domains, dispersed in the ld phase, should be very small (of the order of magnitude of R_0, that is, a few nanometers). On the other hand, domains of ld in the cholesterol-rich end of the coexistence range have a comparatively large size. When the phase boundaries are calculated using Eqs. (15) and (16), very good agreement with the literature is obtained in the cholesterol-rich end (both 0.28 at 30°C), while a considerable larger value is obtained in the cholesterol-poor end (0.18 from RET, compared to ≈0.075 from Ref. 27). These results do not necessarily contradict the published diagram, which was also confirmed by domain size-independent fluorescent measurements [29]. They stem from the distance dependence of RET and the existence of small domains. In other words, there may be phase separation for $x_\alpha < 0.15$, but if this is the case, the domains should be very small. Ideally, the published and RET coexistence boundaries should coincide if the phases are large, as observed at the other end of the tie-line. These observations are probably related to different processes of phase separation, nucleation being preferred in formation of the lo phase from initially pure ld and domain growth being faster in the formation of ld phase from initially pure lo.

MULTICOMPONENT SYSTEMS

Biological membranes are composed of a wide variety of proteins and lipids, so it is tempting to apply RET to systems more complex than those described above (either model membranes with more components or even natural membranes). In this context, Sklar *et al.* [30] studied the thermal phase separation in bovine retinal rod outer segment (ROS) membranes and their phospholipid constituents. Both polarization data and relative quantum yields of parinaric acid fluorescence were reported. The *trans*-parinaric acid partitions preferentially to the gel phase, where it fluoresces much more intensely than in the fluid phase, but its *cis*- isomer does not show a strong preference for any of these phases. In ROS disk membranes, the polarization results are indicative of gel/fluid phase coexistence that disappears before 35°C. At this temperature, only one fluid phase is apparent. When the temperature is lowered, the RET efficiency between *trans*-parinaric and *cis*-retinal added to ROS membrane phospholipids (calculated from the decrease in steady-state intensity of *trans*-parinaric emission) first increases slowly (in our opinion, possibly due to a slight increase in quantum yield and/or decrease in average area per molecule) but, below ~12°C, decreases abruptly. This

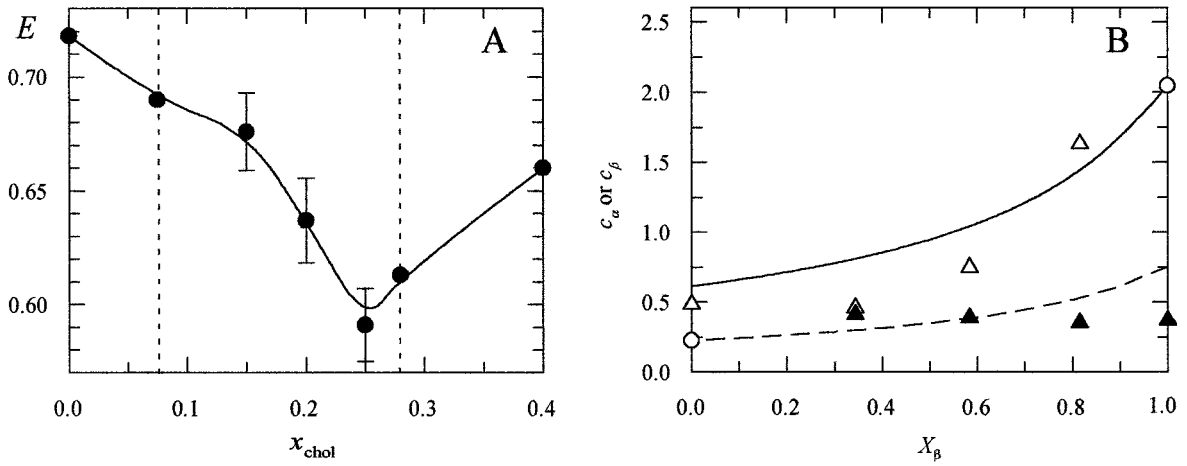

Fig. 4. (**A**) Variation of RET efficiency of NBD-14:0,14:0 PE/Rh-14:0,14:0 PE in 16:0,16:0 PC/cholesterol LUV, as a function of the cholesterol mole fraction, for $T = 30°C$. The error bars' extremes are the results of two measurements. The dashed vertical lines represent the phase coexistence limits according to the phase diagram of Almeida *et al.* [27]. (**B**) Theoretical values (—— and - - -, respectively) and experimental fitting values (△ and ▲, respectively) for the *c* parameters (acceptor concentrations) associated with lo and ld phases (respectively) for NBD-14:0,14:0 PE/Rh-14:0,14:0 PE in 16:0,16:0 PC/cholesterol LUV ($T = 30°C$), as a function of the fraction of lo phase. The open circles represent points where one of the functions c_α or c_β is not defined. Reprinted with permission from Ref. 22. Copyright 2001 Biophysical Society.

result was explained by the partitioning of *trans*-parinaric into the gel phase as it forms and the exclusion of retinal from that phase. To account for the low RET efficiency at low temperatures, the authors proposed that the gel-phase domains should be $>2R_0$, ie., >7 nm. Polarization data indicate that below 20°C some gel-phase clusters have already formed. To be consistent with a still efficient RET at that temperature it was proposed that the gel-phase clusters should be very small. Although a similar trend was observed for RET efficiency from rhodopsin Trp residues to *trans*-parinaric in ROS membranes, when the *cis*-isomer is used, RET is virtually independent of temperature.

RET has been applied to the study of the organization of membranes containing integral proteins, and some interesting models have been developed (albeit some of them are based on assumptions that limit their range of applicability), namely, trying to account for the existence of a "lipid annulus" or lipid belt region surrounding a transmembrane protein with composition and physical properties distinct from those of the bulk lipids [31].

Gutiérrez-Merino [32,33] pioneered analytical expressions for the average rate of energy transfer, $\langle k_T \rangle$. Two specific cases were addressed. First, the case of phase separation in binary phospholipid mixtures (with one component partially labeled with donor and the other component with acceptor, considering a triangular lattice for the lipids in the gel phase) was studied [32]. It was possible to distinguish between gel-phase domains formed from the bulk fluid from the formation of fluid domains from the bulk gel. The second case analyzed was that of random/nonrandom distribution and aggregation state of membrane proteins (assuming RET from a donor in the protein to phospholipids labeled with acceptor [33]). The model includes the relation between $\langle k_T \rangle$ and the size of the domains (whose shape is considered the most compact, i.e., round or hexagonal) in the first case or the relation between $\langle k_T \rangle$ and the geometrical and thermodynamic parameters describing the aggregation of proteins in the second case. Hence, this formalism presents very interesting features. However, there are some limitations to the model, namely, the simplification that underlies the formalism, which consists of considering RET only to the nearest neighbors in the gel-phase lattice (if labeled with acceptor) or from the two external circular layers of the fluid-phase domains (or protein aggregate). On the other hand, the experimental observable being the average RET efficiency given by

$$\langle E \rangle = \left\langle \frac{k_T}{k_T + k_D} \right\rangle \tag{17}$$

where k_D is the donor intrinsic decay rate coefficient, the relation with $\langle k_T \rangle$ is not straightforward. It is proposed that if the setting of experimental conditions is such that the $\langle E \rangle$ is low (namely, $\langle k_T \rangle$ is much smaller than k_D), then $\langle E \rangle \cong \langle k_T \rangle / k_D$. However, low accurate RET efficiencies are difficult to measure experimentally.

This analytical approach was developed by Gutiérrez-Merino *et al.* [34] to calculate $\langle k_T \rangle$ as a function of the

position of the donor in the membrane protein with respect to the plane of acceptors. These approaches were applied to study the lipid annulus around the oligomeric transmembrane acetylcholine receptor (AChR) using RET from the protein Trp residues to 6-lauroyl-2-dimethylaminonaphtalene (laurdan) incorporated in the membrane and comparing the laurdan emission after direct excitation with the sensitized emission after RET from Trp residues [35]. For this purpose, Trp residues were considered to lie in a ring within the perimeter of the transmembrane portion of AChR, and a parameter H (transverse distance between the ring containing donor molecules and the localization of the chromophore in the acceptor molecules) is considered (see Fig. 5). Random and nonrandom distributions of acceptor were considered in the calculation by introducing an apparent dissociation constant of laurdan for the lipid belt region, K_r [33,35].

The lipid belt region was assumed to consist of a unimolecular disk of phospholipids. Another parameter, r, was also considered (distance of closest approach; see Fig. 5). H was allowed to vary between 0 and 10 Å based on previous results, and the simulated curves of $\langle E \rangle$ as a function of acceptor surface density were all fit with $r = 14 \pm 1$ Å. The value of K_r was found to be close to 1. This justifies the goodness of the fits for the previous parameters assuming a random distribution. Had K_r been substantially different from 1, the uncertainty affecting r would probably be much worse. Another question is if there could be a different set of parameters yielding a similarly good fit (because the only criterion is visual inspection of the curves and the data). A global analysis in which several parameters could float simultaneously would circumvent these questions at least partially. In any case, all the conclusions drawn by the authors were cosubstantiated by a wealth of biophysical data on the AChR protein. The laurdan generalized polarizations [36] of emission after direct excitation (reflecting mainly the properties of bulk lipids) and of sensitized emission (after RET, reflecting the properties of the lipid in the immediate vicinity of the receptor, since $R_0 \cong 29$ Å) were compared. Since larger values were found for the latter, especially for the higher temperatures of the large range tested, it was concluded that RET-excited laurdan molecules reside in an environment more rigid than that of the bulk lipid.

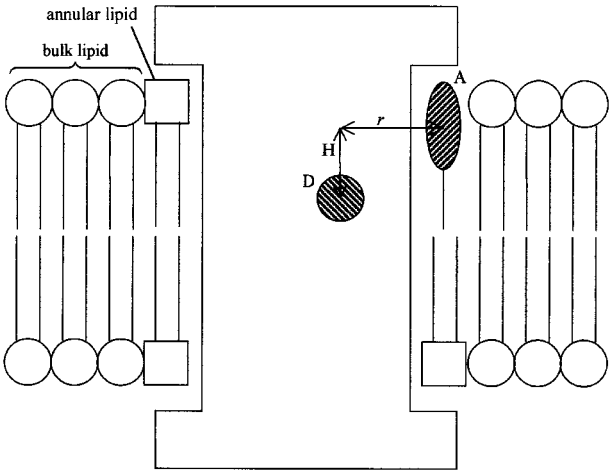

Fig. 5. Schematic representation of a protein embedded in the membrane (e.g., AChR, where a Trp residue acts as a donor, D, to laurdan, A), surrounded by one phospholipid layer of annular lipid (where the acceptors are located). H is the distance between the plane of the donor and that of the acceptor and r is the distance of closest approach between the donor and the acceptor molecules. Adapted from Ref. 35.

Recently, a so-called cluster model was developed to account for RET results in proteoliposomes composed of a mixture of saturated and unsaturated PCs, cholesterol, and rhodopsin [37]. In this model, there is a lipid cluster formed around each protein, with a composition that is different from that of the bulk bilayer, similarly to that described previously. The cluster is characterized by its size (radius R_c; since a round shape is assumed for simplicity) and the partition coefficient of the lipid species between cluster and bulk. These are considered to be two homogeneous phases. The expressions for donor fluorescence decay are given. The difference in average area per lipid molecule in clusters and bulk is omitted, and the acceptor surface density in the lipid clusters is independent of the overall protein/lipid ratio. In this case, the integrated expression (which gives E) is very simple:

$$E = E_c + E_b \tag{18}$$

where E_b is the contribution to the total efficiency from the bulk and E_c from the clusters. The authors use steady-state intensities to calculate E and simulate several curves of E as a function of the acceptor surface density to determine values of the partition coefficient and R_c (those of the curve that best describes the experimental data). Probes were considered to distribute between the two phases as analogue lipids. A value of $R_c = 3.5$ nm was obtained, and since the protein radius is $\approx$2 nm, this corresponds to approximately two layers of annular phospholipid.

Shaklai *et al.* [38] developed a formalism that resulted in simple expressions for the time-resolved and steady-state fluorescence intensity of donors randomly distributed in a plane in the presence of acceptor distributed in another plane, both parallel to the membrane surface. The validity of this model is for the case in which the minimum distance between donor and acceptor (interplanar distance) H is larger than $1.7R_0$. In this situation, the donor decay remains exponential, but with a

shorter lifetime, and an expression analogous to the Stern–Volmer equation for dynamical quenching is obtained for steady-state emission. In the context of this model, there is no possibility of distinguishing between minimum lateral and transversal donor–acceptor distances, and the condition of validity of the model is seldom accomplished [e.g., the authors applied it to RET between 12-(9-anthroyl)-stearic acid and hemoglobin in red blood cell membranes for which $H = 0.91R_0$]. More recently [39] the model was generalized and the range of validity is extended to $H < R_0$. The experimental data presented by Shaklai *et al.* [38] were reanalyzed and a value compatible with the much more complex analysis by Dewey and Hammes [5] was obtained this time. The previous model [38] can be visualized as a cylindrically symmetric labeled protein molecule, with the symmetry axis perpendicular to the plane of the membrane, and assumes that the donor is positioned on the symmetry axis of the protein. In the more recent paper [39] the formulation is extended to the case in which the label is not on the symmetry axis of the protein. Equations for calculating the time-dependent (which are of little use without the simplifications that occur upon integration) and steady-state fluorescence intensities are presented, but methods for applying these theoretical expressions and evaluation of the parameters are discussed only for steady-state data (they result in at least three proximity parameters). The author comments that even in the case of only three parameters to be evaluated by comparison of experimental and theoretical plots, unique values for these parameters cannot be obtained from the experimental plot alone, because there are different sets of parameters that fit the data equally well. One approach to this problem suggested by the author is to assign values to two of the parameters from other types of experiments. The model is used to determine the location of the agonist binding site on the transmembrane AChR in an accompanying paper [40], and an application to an issue in the context of the present review is presented by Dumas *et al.* [41]. In this study, 12:0,12:0 PC/18:0,18:0 DSPC vesicles reconstituted with bacteriorhodopsin (BR) were used. This pair of PCs was chosen for its strongly nonideal mixing behavior and phase equilibria with large regions of gel–fluid and gel–gel phase coexistence in which the two PC species are strongly segregated. Donors were headgroup-labeled NBD-PE with 12:0,12:0 or 18:0,18:0 tails. The acceptor was the retinal group of BR, considered to be located along the symmetry axis of the protein. The distance of closest approach and the interplanar distance were calculated a priori from literature data. The donor quantum yield (and R_0) was calculated for each temperature ($0.45 < H/R_0 < 0.60$). RET efficiency from NBD-12:0,12:0 PE remains practically unchanged (steady and slow decrease) at ~60% up to a temperature of 33°C, above which it drops rapidly, reaching less than 20% above 52°C. An opposite, although less pronounced effect was observed with the probe NBD-18:0,18:0 PE (with a RET efficiency of ~5% at −5°C increasing to ~20% at 25°C, above which it remained unchanged). Polarization of 1,6-diphenylhexatriene shows that the protein in the concentrations used has little influence on the phase equilibria of the binary lipid mixture. The following interpretation (consistent with theoretical calculations) was given. At low temperatures, when two gel phases coexist, BR is associated with the short-chain 12:0,12:0 PC. At moderate temperatures, in the gel–fluid coexistence region, BR remains associated with 12:0,12:0 PC, the major component of the fluid, but is enriched at the interface between the gel and the fluid domains. At high temperatures, BR remains in the single fluid phase, but a preference for the long-chain 18:0,18:0 PC molecules at the expense of the short-chain 12:0,12:0 PC (reflecting the hydrophobic matching) is suggested.

Wang *et al.* [42] used RET from Trp residues of gramicidin (an ionophore peptide) to different classes of phospholipids (PC, PE, PA) labeled with 5-(dimethylamino)naphtalene-1-sulfonyl (dansyl) and showed that all of the phospholipids employed were randomly distributed in the egg yolk PC/PE/PA mixture. The recovered R_0 values for the pairs gramicidin (Trp)/dansyl-labeled phospholipid were very close to the values obtained through Eq. (2). The addition of Ca^{2+} (4.5 m*M*) to egg PC/PA vesicles caused an appreciable increase in dansyl-PA polarization, although the polarization of dansyl-PC remained unaffected. This observation can be interpreted as a Ca^{2+}-induced phase separation, with the formation of a new gel-like phase rich in PA, stabilized by Ca^{2+}. Accordingly, a considerable increase in RET efficiency from gramicidin to dansyl-PC and a decrease in RET efficiency to dansyl-PA were observed. In principle, this means also that gramicidin has a preference for the fluid PC-rich phase. If the enzyme D-β-hydroxibutirate dehydrogenase is used instead of gramicidin, then the lipid distribution is changed even in the absence of Ca^{2+}. The RET efficiency from the enzyme Trp residues to the labeled lipids decreases in the order dansyl-PA, -PC, and -PE. It is noteworthy that the enzyme activity requires the presence of PC but it is much more efficiently reconstituted in vesicles containing anionic phospholipid.

Glaser and co-workers also studied domain formation in the presence of vesicular stomatitis virus (VSV) envelope proteins, by comparing fluorescence microscopy and RET results [43,44]. These studies have significant biological relevance, because viruses of the same

class as VSV bud from domains of the plasma membrane that have a unique protein and lipid composition, and the underlying mechanisms are relatively unknown. For example, to observe sphingomyelin-enriched domains in the fluorescence microscopy images of 18:1,18:1 PC unilamellar vesicles (from NBD-sphingomyelin fluorescence), the presence of both virus envelope proteins (G and M) and also PA was required. The RET efficiency from G-protein Trp residues to dansyl-sphingomyelin was measured. In accordance with the microscopy results, only when G and M proteins and PA were present was an efficiency higher than that observed for control egg-PC vesicles (containing only G protein and dansyl-PC; random distribution) measured. These are qualitative studies using steady-state fluorescence but illustrate well the potentialities of applying RET to biologically relevant problems involving membranes.

Recently, a new form of digital microscopy, RET imaging, was developed [45]. Using this technique, the authors studied the clustering of GPI-anchored proteins, specifically 5′-nucleotidase (5′-NT) in the apical membrane of Madin–Darby canine kidney (MDCK) cells, thought to be associated with sphingolipid and cholesterol in lipid rafts [46]. Antibodies labeled with either donor or acceptor were employed, providing a simple way to vary the surface density of either probe. RET efficiency was determined by photobleaching the acceptor. This method has the advantage of using the same sample to obtain the fluorescence intensity in the presence and absence of acceptor. To carry out the measurements, one region of interest per cell was chosen, and the mean fluorescence intensities of donor and acceptor and RET efficiencies were averaged over 40×40 pixels. The mean fluorescence intensity in the averaged area is proportional to the mean concentration, and since a calibration procedure was used, it was possible to obtain the mean surface density of donor and acceptor for each averaged area. In this way, E was represented as a function of the acceptor surface density or donor surface density, showing that it decreases to zero for a low acceptor surface density and is independent within a reasonable range of donor surface density. These data were consistent with theoretical predictions for two-dimensional RET for randomly distributed molecules, which indicates that most 5′-NT molecules are not clustered over $< 2R_0 = 10$ nm. The consequence of this result for the structure of lipid rafts is that either they are very small or, alternatively, they comprise the entire apical membrane. The authors estimated that the lower limit of detection is approximately 20% clustered/80% randomly distributed. Supposing that 10% of the membrane (molar ratio) is in the "raft phase," and the partition coefficient [Eq. (12)] of the GPI-anchored protein between the raft and the nonraft phases is 3, then only 25% of the protein would be inside the rafts, just within the lower limit of detection. In an attempt to correlate these results with those of other authors, namely, those using detergent extraction [46], and the experiment of Varma and Mayor (which reported clustering in domains with less than 70 nm of a GPI-anchored protein [47]), RET imaging studies were extended to a variety of cell types and raft markers [48]. To explain the inability to detect clustering of any such markers, even ganglioside M1 (detected due to its strong binding to fluorescently labeled cholera toxin B), several arguments were presented in addition to the one discussed above. Fundamentally, the rafts would be so small that the probes would be relatively large, preventing simultaneous binding of probes to adjacent raft markers, or they would exist only as transiently stabilized structures. Also recently, in a high-resolution single-particle tracking study in a similar system [49], the radius of rafts was estimated as 26 ± 13 nm (but even one cell might have a distribution of sizes, and the size of a single raft might be dynamic). These examples show that the characterization of lipid rafts is a very active research subject, in which there are not yet conclusive answers, and RET should be a powerful tool in this respect.

CONCLUDING REMARKS

The recovery of information of a more quantitative nature will demand the measurement of high-quality fluorescence decay data, because the decay curve is very sensitive to nonrandom distribution effects, which may not be clear in the steady-state measurement (integration of the decay over time). Moreover, time-resolved measurements of the donor decay are not affected by common steady-state artifacts, such as inner filter or reabsorption effects. On the other hand, steady-state RET measurements may reveal static quenching phenomena (through formation of donor–acceptor complexes) and should still be carried out. The two types of measurements are thus complementary. In any case, the decay contains a superior amount of information, and only the unavailability of high-quality equipment at reasonable prices and fast computers for complex decay analysis may justify the far greater number of literature steady-state RET studies. Due to the recent progress in both these aspects, this situation may well be changing.

Some care in planning RET experiments should, nevertheless, always be taken. One example is the use of analogue probes, i.e., fluorescent probes that mimic a nonfluorescent molecule for which membrane behavior

information is intended. A priori, it should not be expected that the probe behaves exactly like the parent molecule, and literature examples are becoming more and more common. The random distribution/aggregation tendency of probes in single-phase systems should be verified. The partition coefficients between the phases should be known or determined. For this matter, it is important to work over a tie-line, which is immediate in a binary system if the phase boundaries are known but may well be tricky in higher-order systems.

RET is very promising for the study of lo/ld systems (which seems to be similar to the case of raft heterogeneity), because DSC is insensitive to these transitions, and detergent extraction alters the initial composition of the phases. Nevertheless, to obtain the maximum of quantitative information, the area per lipid molecule has to be known, as well as the transverse location of the fluorophore. An important effect should be that of cholesterol, which changes not only the average area/per phospholipid molecule but also the bilayer hydrophobic thickness.

ACKNOWLEDGMENTS

This work was funded by Program PRAXIS XXI, FCT, Portugal. R.F.M.A. acknowledges a grant from PRAXIS XXI (BD 943/2000).

REFERENCES

1. S. J. Singer and G. L. Nicolson (1972) *Science* **175**, 720–731.
2. O. G. Mouritsen and K. Jørgensen (1997) *Curr. Opin. Struct. Biol.* **7**, 518–527.
3. L. Davenport (1997) *Methods Enzymol.* **278**, 487–512.
4. B. Van Der Meer, G. Coker, III, and S.-Y. S. Chen (1994) *Resonance Energy Transfer: Theory and Data*, VCH, New York.
5. T. G. Dewey and G. G. Hammes (1980) *Biophys. J.* **32**, 1023–1036.
6. A. Polozova and B. J. Litman (2000) *Biophys. J.* **79**, 2632–2643.
7. Th. Förster (1949) *Z. Naturforsch.* **4a**, 321–327.
8. L. Davenport, R. E. Dale, R. H. Bisby, and R. B. Cundall (1985) *Biochemistry* **24**, 4097–4108.
9. P. K. Wolber and B. S. Hudson (1979) *Biophys. J.* **28**, 197–210.
10. B. K. Fung and L. Stryer (1978) *Biochemistry* **17**, 5241–5248.
11. K. Kano, H. Kawazumi, and T. Ogawa (1981) *J. Phys. Chem.* **85**, 2998–3003.
12. N. Tamai, T. Yamazaki, I. Yamazaki, A. Mizuma, and N. Mataga (1987) *J. Phys. Chem.* **91**, 3503–3508.
13. I. Yamazaki, N. Tamai, and T. Yamazaki (1987) *J. Phys. Chem.* **94**, 516–525.
14. P. M. Ballet, M. Van der Auweraer, F. C. De Schryver, H. Lemmetyinen, and E. Vourimaa (1996) *J. Phys. Chem.* **100**, 13701–13715.
15. G. Lantzsch, H. Binder, and H. Heerklotz (1994) *J. Fluoresc.* **4**, 339–343.
16. L. M. S. Loura, A. Fedorov, and M. Prieto (1996) *Biophys. J.* **71**, 1823–1836.
17. Y. S. Liu, L. Li, S. Ni, and M. Winnik (1993) *Chem. Phys.* **177**, 579–589.
18. L. M. S. Loura and M. Prieto (2000) *J. Phys. Chem. B* **104**, 6911–6919.
19. D. W. Marquardt (1963) *J. Soc. Ind. Appl. Math. (SIAM J.)* **11**, 431–441.
20. L. M. S. Loura, A. Fedorov, and M. Prieto (2000) *J. Phys. Chem. B* **104**, 6920–6931.
21. L. M. S. Loura, M. A. R. B. Castanho, A. Fedorov, and M. Prieto (2001) *Biochim. Biophys. Acta* **1510**, 125–135.
22. L. M. S. Loura, A. Fedorov, and M. Prieto (2001) *Biophys. J.* **80**, 776–778.
23. W. Stillwell, L. J. Jenski, M. Zerouga, and A. C. Dumaual (2000) *Chem. Phys. Lipids* **104**, 113–132.
24. L. M. S. Loura, A. Fedorov, and M. Prieto (2000) *Biochim. Biophys. Acta* **1467**, 101–112.
25. O. G. Mouritsen and M. Bloom (1984) *Biophys. J.* **46**, 141–153.
26. T. Ahn and C.-H. Yun (1998) *J. Biochem (Tokyo)* **124**, 622–627.
27. P. F. F. Almeida, W. L. C. Vaz, and T. E. Thompson (1992) *Biochemistry* **31**, 6739–6747.
28. L. M. S. Loura, A. Fedorov, and M. Prieto (2001) *Biochim. Biophys. Acta* **1511**, 236–243.
29. C. R. Mateo, A. U. Acuña, and J.-C. Brochon (1995) *Biophys. J.* **68**, 978–987.
30. L. A. Sklar, G. P. Miljanich, S. L. Bursten, and E. A. Dratz (1979) *J. Biol. Chem.* **254**, 9583–9591.
31. D. Marsh and F. J. Barrantes (1978) *Proc. Natl. Acad. Sci. USA* **75**, 4329–4333.
32. C. Gutiérrez-Merino (1981) *Biophys. Chem.* **14**, 247–257.
33. C. Gutiérrez-Merino (1981) *Biophys. Chem.* **14**, 259–266.
34. C. Gutiérrez-Merino, F. Munkonge, A. M. Mata, J. M. East, B. L. Levinson, R. M. Napier, and A. G. Lee (1987) *Biochim Biophys Acta* **897**, 207–216.
35. S. S. Antollini, M. A. Soto, I. Bonini de Romanelli, C. Gutiérrez-Merino, P. Sotomayor, and F. J. Barrantes (1996) *Biophys. J.* **70**, 1275–1284.
36. T. Parasassi, G. De Stasio, A. d'Ubaldo, and E. Gratton (1990) *Biophys. J.* **57**, 1179–1186.
37. A. Polozova and B. J. Litman (2000) *Biophys. J.* **79**, 2632–2643.
38. N. K. Shaklai, J. Yguerabide, and H. M. Ranney (1977) *Biochemistry* **16**, 5585–5592.
39. J. Yguerabide (1994) *Biophys. J.* **66**, 683–693.
40. C. F. Valenzuela, P. Weign, J. Yguerabide, and D. A. Johnson (1994) *Biophys. J.* **66**, 674–682.
41. F. Dumas, M. M. Sperotto, M. C. Lebrun, J. F. Tocanne, and O. G. Mouritsen (1997) *Biophys. J.* **73**, 1940–1953.
42. S. Wang, E. Martin, J. Cimino, G. Omann, and M. Glaser (1988) *Biochemistry* **27**, 2033–2039.
43. P. Luan and M. Glaser (1994) *Biochemistry* **33**, 4483–4489.
44. P. Luan, L. Yang, and M. Glaser (1995) *Biochemistry* **34**, 9874–9883.
45. A. K. Kenworthy and M. Edidin (1998) *J. Cell Biol.* **142**, 69–84.
46. E. London and D. A. Brown (2000) *Biochim. Biophys. Acta* **1508**, 182–195.
47. R. Varma and S. Mayor (1998) *Nature* **394**, 798–801.
48. A. K. Kenworthy, N. Petranova, and M. Edidin (2000) *Mol. Biol. Cell* **11**, 1645–1655.
49. A. Pralle, P. Keller, E. L. Florin, K. Simons, and J. K. Horber (2000) *J. Cell Biol.* **148**, 997–1007.